

1    **Insights into overall photocatalytic water**  
2    **splitting through simultaneous *in situ* H<sub>2</sub>**  
3    **and O<sub>2</sub> measurements**

4    **Authors:** Nadzeya Brezhneva,<sup>1,2</sup> Alexander Eith,<sup>1,2</sup> Ebrahim Abedini,<sup>1,2</sup> Daniel Kowalczyk,<sup>3</sup> Dirk  
5    Ziegenbalg,<sup>3</sup> Jacob Schneidewind<sup>1,2,4,5\*</sup>

6    **Affiliations:**

7        1 Institute of Organic Chemistry and Macromolecular Chemistry, Friedrich Schiller University  
8        Jena, Humboldtstraße 10, 07743 Jena, Germany

9        2 Center for Energy and Environmental Chemistry Jena (CEEC Jena), Friedrich Schiller  
10      University Jena, Philosophenweg 7a, 07743 Jena, Germany

11      3 Institute of Chemical Engineering, Ulm University, Albert-Einstein-Allee 11, 89081 Ulm,  
12      Germany

13      4 Jena Center for Soft Matter (JCSM), Friedrich Schiller University Jena, Philosophenweg 7,  
14      07743 Jena, Germany

15      5 Helmholtz Institute for Polymers in Energy Applications Jena (HIPOLE Jena), Lessingstrasse  
16      12-14, 07743 Jena, Germany

17      \*Corresponding author, e-mail: Jacob.Schneidewind@uni-jena.de

18    **ORCID:**

Nadzeya Brezhneva	0009-0005-5516-0380
Alexander Eith	0000-0003-3413-8342
Ebrahim Abedini	0000-0002-6469-8781
Daniel Kowalczyk	0000-0002-3603-5980
Dirk Ziegenbalg	0000-0001-6104-4953
Jacob Schneidewind	0000-0002-5328-6626

20 **Keywords:** Photocatalysis, water splitting, hydrogen, in situ measurements, photoreactor, kinetics

21 **This file includes:**

22 Table of contents entry

23 Abstract

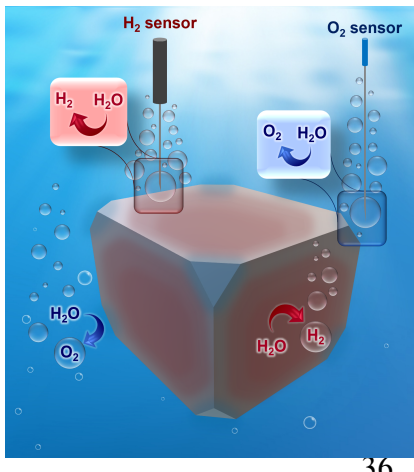
24 Main text

25 Figures 1 to 3

26 Acknowledgements, funding, author contributions, data and code availability, competing  
27 interests, correspondence and supplementary materials statements

28 References

29 **Table of Contents Entry**



A photoreactor set-up allowing for simultaneous *in situ* detection of H<sub>2</sub> and O<sub>2</sub> in the liquid as well as gas phase is described. Using this system, overall water splitting with Rh<sub>2-y</sub>Cr<sub>y</sub>O<sub>3</sub>/Al:SrTiO<sub>3</sub> is investigated, determining irradiance dependence, thermal activation barrier, optimal co-catalyst loading and H/D kinetic isotope effect.

36

37

38 .

39 **Abstract**

40 Photocatalytic overall water splitting is a promising pathway to green hydrogen but also presents  
41 unique research challenges due to the need to detect both gaseous products ( $H_2$  and  $O_2$ ). While gas  
42 chromatography (GC) is the most commonly employed method in this context, it faces multiple  
43 shortcomings: low time resolution as well as the need to alter the reaction conditions (vacuum or inert  
44 gas flushing) to feed the products in to the GC, which limits the extent to which obtained insights can  
45 be translated into scalable photoreactors (where  $H_2$  and  $O_2$  accumulate). Against this backdrop we  
46 report a novel photoreactor set-up which allows for simultaneous *in situ* detection of  $H_2$  and  $O_2$  in both  
47 the liquid and gas phase. It is based on a standardized modular photoreactor platform, fully open source  
48 and allows for reproducible measurements. Using this set-up, we investigate photocatalytic overall  
49 water splitting using  $Rh_{2-y}Cr_yO_3/Al:SrTiO_3$ , determining the irradiance dependence, thermal activation  
50 barrier, optimal co-catalyst loading and H/D kinetic isotope effect. This highlights the versatility of  
51 the set-up as well as the depth of information that can be obtained through the *in situ*  $H_2/O_2$  detection  
52 approach.

53

54 **Introduction**

55 Photocatalytic overall water splitting, wherein water is split into hydrogen and oxygen, offers a  
56 promising route for the scalable conversion of sunlight to green hydrogen.<sup>[1–3]</sup> Various photocatalysts  
57 have been developed for this reaction, largely based on semiconductors such as TiO<sub>2</sub>,<sup>[4]</sup> SrTiO<sub>3</sub>,<sup>[5]</sup>  
58 C<sub>3</sub>N<sub>4</sub><sup>[6]</sup> and others.<sup>[7]</sup> A crucial aspect of photocatalytic overall water splitting research, and thus a  
59 prerequisite for further progress in the field, is the reliable detection of the two reaction products, H<sub>2</sub>  
60 and O<sub>2</sub>. Aside from indicating the catalyst's activity, quantification of both gases gives insights into  
61 whether the reaction really does occur stoichiometrically (forming the expected 2:1 H<sub>2</sub>/O<sub>2</sub> ratio) and  
62 can give insights into the reaction kinetics.<sup>[8,9]</sup> The vast majority of published works employ gas  
63 chromatography (GC) to quantify H<sub>2</sub> and O<sub>2</sub> in the gas phase, often in a closed gas circulation system  
64 allowing for online measurements.<sup>[8,9]</sup>

65 While this approach has been widely employed, it also presents multiple challenges: 1) The entire  
66 photocatalytic set-up is complex and relatively expensive (especially due to the GC component),  
67 creating challenges for accessibility and high-throughput work. 2) The use of a GC typically requires  
68 either flushing the reaction solution with an inert carrier gas or operating it under vacuum to feed the  
69 product gases into the system. These interventions often positively impact photocatalytic performance,  
70 since overall water splitting systems generally show higher activity under reduced background  
71 pressure and in the absence of H<sub>2</sub>/O<sub>2</sub> in the gas phase.<sup>[10]</sup> However, those conditions are not  
72 representative of scalable photoreactor systems, where H<sub>2</sub> and O<sub>2</sub> accumulate in the gas phase.<sup>[3]</sup> 3)  
73 The time resolution of GC is limited, usually on the scale of minutes. This low time resolution limits  
74 the kinetic insights that can be gained, since the long measurement time scales conflate intrinsic kinetic  
75 effects (e.g. temperature dependence) with slower processes (e.g. catalyst degradation).<sup>[11]</sup> This is  
76 compounded by the fact that gas phase measurements cannot provide insights into the initial reaction  
77 phase, since H<sub>2</sub> and O<sub>2</sub> are initially formed in the liquid phase and must diffuse into the gas phase  
78 before they can be detected. Alternative methods to GC have been reported in the literature, such as  
79 electrochemical or optical sensing of O<sub>2</sub>,<sup>[12–14]</sup> and in the context of photoelectrochemical water

80 splitting, H<sub>2</sub> has also been detected *in situ* using electrochemical microsensors.<sup>[15,16]</sup> However, such  
81 approaches have, to the best of our knowledge, not been applied in overall photocatalytic water  
82 splitting.

83 A second challenge for photocatalysis research is the reproducibility of experiments, since  
84 photocatalytic reactions are highly sensitive to the precise irradiation parameters.<sup>[8]</sup> Progress has been  
85 made on the development of standardized modular photoreactor platforms,<sup>[17]</sup> but there is still a strong  
86 need for reproducible experimental set-ups to facilitate comparisons between photocatalysts and  
87 enable structured progress in the field.<sup>[18,19]</sup>

88 Against this backdrop, we are introducing a novel photoreactor set-up based on a standardized modular  
89 reactor platform with simultaneous *in situ* detection of H<sub>2</sub> and O<sub>2</sub> in both the gas and liquid phase. This  
90 low-cost, fully open-source, documented and reproducible system allows for precise control of all  
91 relevant reaction conditions (irradiance, temperature, gas phase composition) and does not require any  
92 carrier gases or changes to the reaction conditions. It therefore allows for the collection of  
93 photocatalytic performance data under true *operando* conditions that are directly relevant to scalable  
94 photoreactor systems. Importantly, the highly time-resolved measurements (on the level of seconds)  
95 of H<sub>2</sub> and O<sub>2</sub> give rich kinetic insights in both the gas and liquid phase. This provides information on  
96 the initial reaction phase, which allows for precise determination of the kinetic influence of reaction  
97 parameters (irradiance, temperature etc.) without conflating them with slower processes such as  
98 catalyst degradation. We use this set-up to investigate overall water splitting using the previously  
99 reported Rh<sub>2-y</sub>Cr<sub>y</sub>O<sub>3</sub>/Al:SrTiO<sub>3</sub> photocatalyst,<sup>[20-22]</sup> studying the influence of temperature, irradiance  
100 and co-catalyst loading on the initial reaction rate in the liquid phase and measuring the H/D kinetic  
101 isotope effect (KIE). Through these investigations, we find that liquid phase measurements can  
102 reproduce previously reported reactivity trends while also providing new insights that require further  
103 investigations, such as a H/D KIE which is, surprisingly, higher than previously reported.

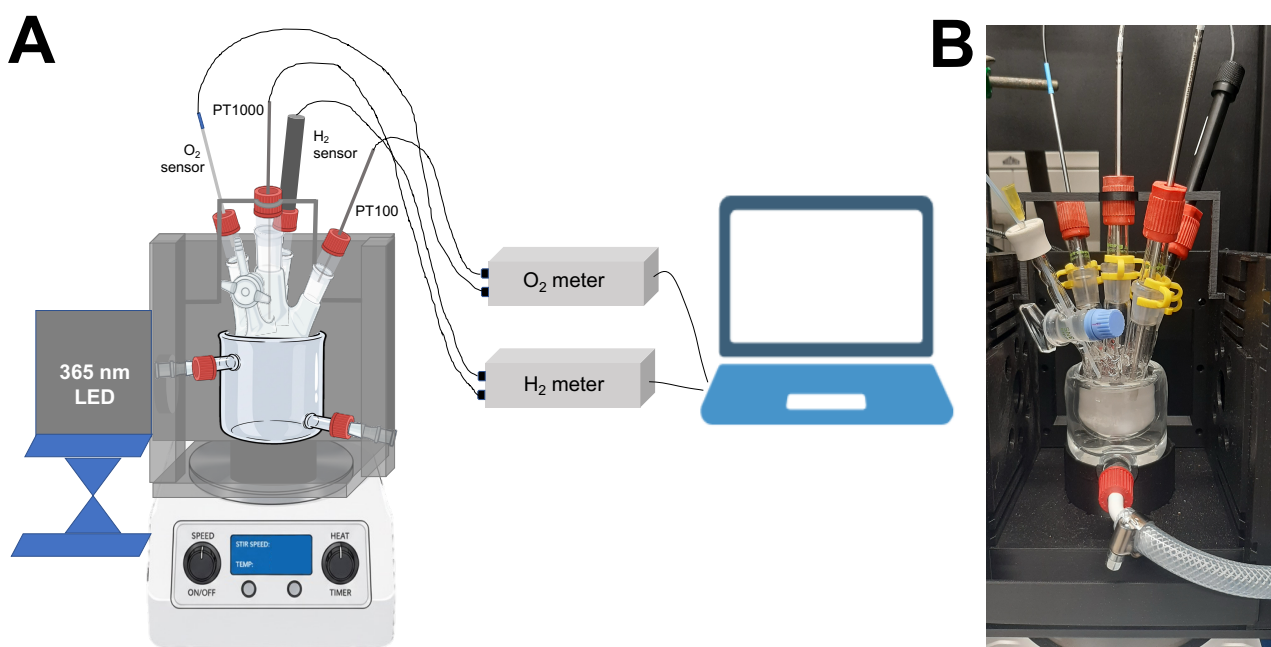
104

105 **Results and Discussion**

106 **Photocatalytic reactor set-up**

107 The goal for the photocatalytic reactor set-up is to offer precise control over irradiance, temperature  
108 and the composition of the gas phase while also allowing for *in situ* detection of H<sub>2</sub> and O<sub>2</sub>. To address  
109 the control of the reaction conditions and also expand on a standardized modular reaction platform,  
110 we modified the previously reported modular photoreactor design.<sup>[17]</sup> Based on this design, we created  
111 the 3D printed irradiation chamber (see Figure 1), which allows for precise placement of light source  
112 and reactor, keeping all distances constant so as to enable reproducible irradiation experiments (since  
113 irradiance strongly varies with distance from the light source).

114



115 Figure 1 **A** Schematic overview of light source (365 nm LED), 3D printed irradiation chamber (black), double walled  
116 beaker for temperature control, glass photoreactor and H<sub>2</sub> as well as O<sub>2</sub> sensors with temperature probes for compensation.  
117 **B** Photo of experimental set-up.

118 The irradiation chamber also allows for the incorporation of a double walled beaker, which is  
119 connected to a thermostat to precisely control the reaction temperature. This is crucial to both avoid  
120 inadvertent heating of the reactor due to irradiation and to enable the reaction to be performed at

121 different set temperatures to study the temperature dependence of the water splitting reaction. The  
122 reaction is performed in a glass Schlenk photoreactor, which has four glass connections as well as a  
123 valve. Being a Schlenk flask, the gas composition can be precisely controlled using standard Schlenk  
124 technique (e.g. applying vacuum, filling with an inert gas or filling with a defined H<sub>2</sub>/O<sub>2</sub> mixture). The  
125 four glass connections allow for the installation of up to four sensors for H<sub>2</sub> and O<sub>2</sub> detection. In this  
126 study, we have utilized an electrochemical H<sub>2</sub> microsensor and an optical O<sub>2</sub> sensor. As the  
127 measurement signals of both sensors are sensitive to temperature, temperature sensors are also installed  
128 in the reactor to provide real-time temperature compensation. All sensors are connected to the  
129 respective H<sub>2</sub>/O<sub>2</sub> meters, which read out the signal and provide the data to a computer. Importantly,  
130 the used sensors can be applied in both the gas and liquid phase (by adjusting their position within the  
131 reactor), allowing for studying product formation in both phases. To ensure precise measurement of  
132 H<sub>2</sub> and O<sub>2</sub> in the set-up, both sensors were carefully calibrated before all experiments. For more  
133 information see supporting information (SI) section 5. The reaction solution is stirred using a magnetic  
134 stirring bar, ensuring homogeneous distribution of photocatalyst particles and avoiding local  
135 concentration differences.

136 Detailed information on the used components can be found in SI section 4, and the data repository  
137 contains all necessary files for 3D printing, allowing other researchers to replicate this experimental  
138 set-up.

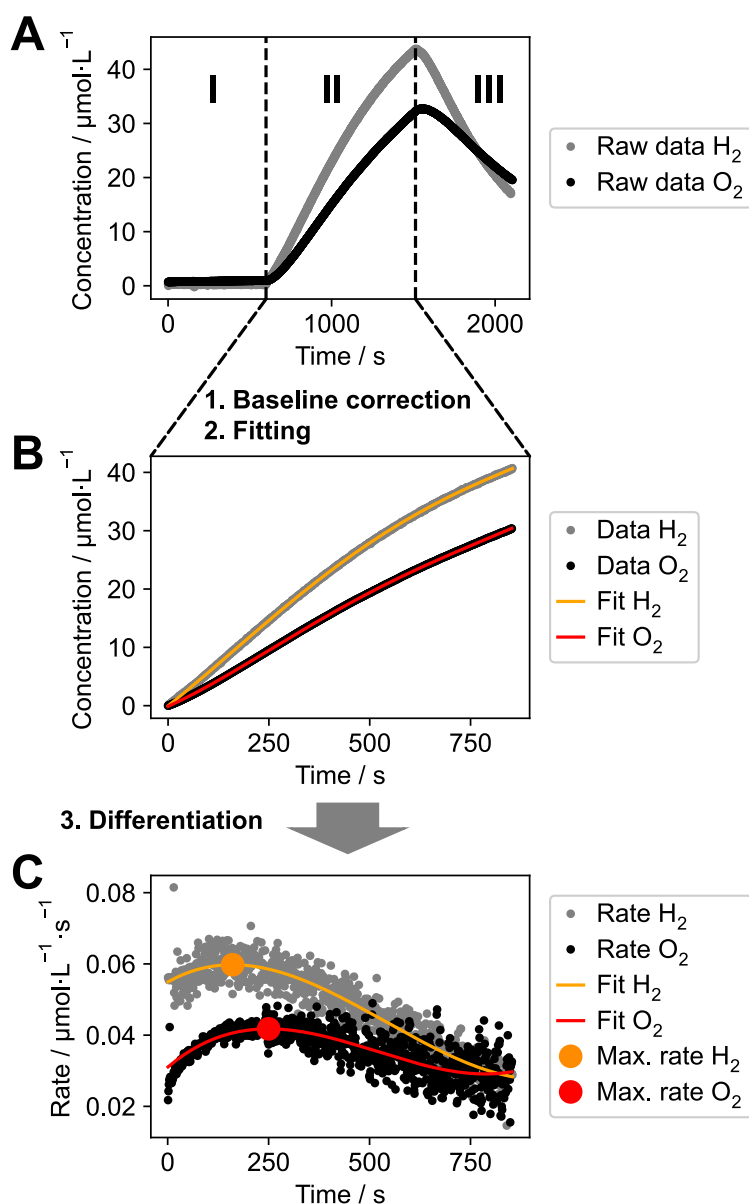
### 139 **Photocatalytic reaction system**

140 To investigate photocatalytic overall water splitting using the described reactor set-up, we prepared a  
141 previously reported Rh<sub>2-y</sub>Cr<sub>y</sub>O<sub>3</sub>/Al:SrTiO<sub>3</sub> photocatalyst,<sup>[5,20,21]</sup> adapting a procedure from Osterloh  
142 and co-workers (see SI section 3).<sup>[22]</sup> This photocatalyst is composed of aluminum-doped SrTiO<sub>3</sub>  
143 particles (size range of 500 – 2000 nm, see SI section 3.6), which are loaded with a mixed  
144 rhodium/chromium oxide (typically 0.1 wt.% Rh/Cr). The Al:SrTiO<sub>3</sub> particles serve as light absorbers,  
145 while the Rh<sub>2-y</sub>Cr<sub>y</sub>O<sub>3</sub> particles serve as co-catalysts for the hydrogen evolution reaction.<sup>[20]</sup> This

146 catalyst is known to stoichiometrically split water into H<sub>2</sub> and O<sub>2</sub> when irradiated with UV light (e.g.  
147 365 nm) in an aqueous suspension.<sup>[20,22]</sup>

## 148 Data processing workflow

149 With both the photoreactor set-up and catalyst in hand, we collected the experimental data and  
150 established a corresponding data processing workflow (see Figure 2).



151 Figure 2 Workflow for the processing of experimentally collected H<sub>2</sub>/O<sub>2</sub> data, illustrated for liquid phase data (processing  
152 is performed analogously for gas phase data). **A** Raw liquid phase data for H<sub>2</sub>/O<sub>2</sub>, showing the three experiment phases: I)  
153 pre-reaction baseline, II) reaction phase (irradiation), III) post-reaction phase, showing diffusion of gases in to the gas  
154 phase. **B** Reaction phase data which is baseline corrected and the start of irradiation is set to  $t=0$  s. Furthermore, polynomial

155 fits to the data are shown. C Numerically differentiated rate data along with the differentiated polynomial fit, from which  
156 the maximum rates of H<sub>2</sub> and O<sub>2</sub> are determined. Note: the shown rate data is based on numerical differentiation of  
157 experimental data which has been smoothed using a Savitzky-Golay filter to reduce the noise level for visualization. Details  
158 on the data processing workflow can be found in SI section 8.1.

159 The collected raw data can be divided into three phases (see Figure 2A): I) the pre-reaction baseline  
160 before irradiation is turned on, II) reaction phase, during which irradiation is turned on and III) the  
161 post-reaction phase (irradiation turned back off again). For liquid phase measurements, it can be  
162 observed that the gas concentration decreases during this phase due to diffusion into the gas phase (see  
163 Figure 2A).

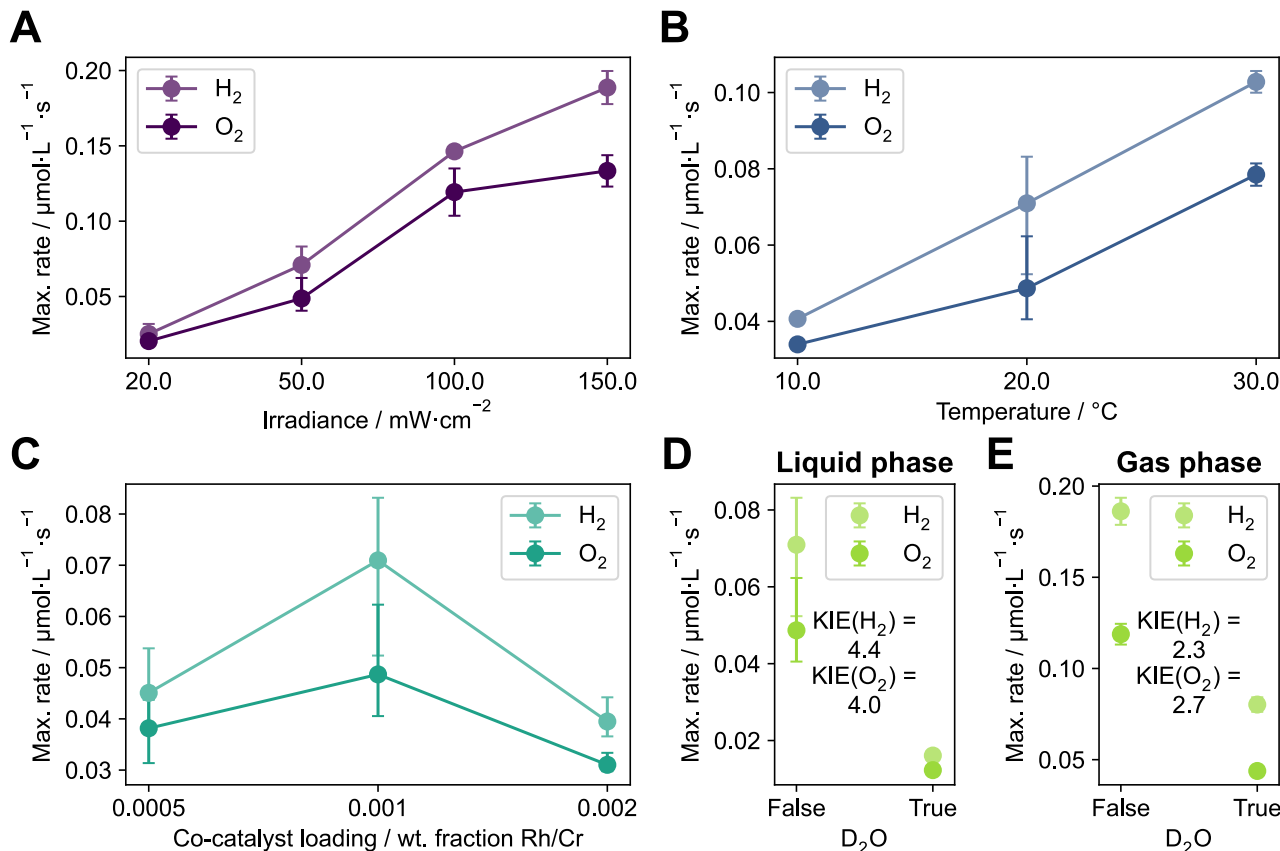
164 The reaction phase is selected for further processing, based on the start and end time of the irradiation,  
165 and baseline corrected as well as shifted on x-axis so that the start of the reaction is at  $t = 0$  s. The first  
166 60 s after the start of the irradiation are removed in this step as this period is typically strongly affected  
167 by diffusion of gases into the sensors as well as artefacts arising from the small ( $< 0.5$  °C) but sudden  
168 temperature change due to warming by the irradiation. To the reaction phase data (Figure 2B), a  
169 polynomial is fitted. This smooth polynomial allows for accurate extraction of rate data upon  
170 numerical differentiation (see Figure 2C), as the experimental data is quite noisy after differentiation.  
171 For this study, the key kinetic information we use for the analysis of experiments is the maximum rate,  
172 which is determined by picking the maximum value of the differentiated polynomial fit (see Figure  
173 2C). The maximum rate is used as a proxy for the initial rate, which itself cannot be determined directly  
174 due to diffusion of gases into the sensor at the beginning of the reaction, which leads to a short  
175 induction period.

176 However, as the full temporal evolution of concentration and rates is available, other kinetic  
177 information can be obtained from the data, for example by fitting full kinetic models.

178 The observed ratio of H<sub>2</sub>/O<sub>2</sub> varies during the course of the experiment and only converges slowly to  
179 the expected 2:1 ratio in the gas phase. In SI section 8.2 we provide a simple phenomenological model  
180 to rationalize this observation based on the different solubilities of H<sub>2</sub> and O<sub>2</sub> in water.

181    **Kinetic investigation of overall photocatalytic water splitting using Rh<sub>2</sub>  
182    yCr<sub>y</sub>O<sub>3</sub>/Al:SrTiO<sub>3</sub>**

183    With the data processing workflow established, we performed a series of experiments using the Rh<sub>2</sub>  
184    yCr<sub>y</sub>O<sub>3</sub>/Al:SrTiO<sub>3</sub> photocatalyst. Initially, we established the reproducibility of the experimental and  
185    data processing protocol by testing the reference conditions ( $T = 20\text{ }^{\circ}\text{C}$ ,  $50\text{ mW}\cdot\text{cm}^{-2}$  irradiance, 0.1  
186    wt.% Rh/Cr loading) seven times with liquid phase measurements. This gave maximum rates of H<sub>2</sub>  
187    and O<sub>2</sub> formation of  $0.07 \pm 0.01\text{ }\mu\text{mol}\cdot\text{L}^{-1}\cdot\text{s}^{-1}$  and  $0.05 \pm 0.009\text{ }\mu\text{mol}\cdot\text{L}^{-1}\cdot\text{s}^{-1}$  (error bars are standard  
188    deviations) in the liquid phase respectively, showing good reproducibility of the measurements.  
189    Next, we varied three experimental parameters to study their influence on the maximum rates in the  
190    liquid phase: irradiance, temperature and co-catalyst loading (see Figure 3A-C).



191    Figure 3 Impact of different experimental parameters on the maximum rates of H<sub>2</sub>/O<sub>2</sub> formation (in the liquid phase, unless  
192    indicated otherwise). **A** Variation of irradiance. **B** Variation of reaction temperature. **C** Variation of co-catalyst loading. **D**  
193    & **E** Performing the reaction in either H<sub>2</sub>O or D<sub>2</sub>O to measure the kinetic isotope effect (KIE) using both liquid and gas  
194    phase measurements. The KIE is calculated both on the ratios of the maximum rates of H<sub>2</sub> and O<sub>2</sub> formation. For all figures:

195 shown error bars indicate the maximum and minimum rates obtained during experiments. The underlying experimental  
196 data is shown fully in SI section 8.3.

197 Varying the irradiance from 20 to 150 mW·cm<sup>-2</sup> (Figure 3A), we observed a roughly linear increase  
198 of the maximum rate. This first order dependence on irradiance is consistent with previous findings  
199 based on gas phase measurements.<sup>[20,23]</sup>

200 Increasing the temperature in the range of 10 – 30 °C also results in an increase of the maximum rates  
201 (see Figure 3B), which indicates that there are rate limiting thermal reaction steps involved in the  
202 photocatalytic reaction sequence, consistent with previous findings.<sup>[21,24]</sup> We performed an Arrhenius  
203 analysis (see SI section 8.4) of the temperature dependent data and found thermal activation barriers  
204 of  $33.1 \pm 3.2 \text{ kJ}\cdot\text{mol}^{-1}$  and  $29.9 \pm 3.0 \text{ kJ}\cdot\text{mol}^{-1}$  based on the H<sub>2</sub> and O<sub>2</sub> data, respectively.

205 Varying the loading of the Rh<sub>2-y</sub>Cr<sub>y</sub>O<sub>3</sub> co-catalyst between 0.05 – 0.2 wt.% (0.0005 – 0.002 wt.  
206 fraction, see Figure 3C) shows that the optimal loading is at 0.1 wt.%, being also consistent with  
207 previous studies.<sup>[23]</sup>

208 Finally, we performed the reaction also in D<sub>2</sub>O to measure the H/D kinetic isotope effect (KIE, see  
209 Figure 3D and E). First, we performed the reaction with liquid phase measurements, finding KIEs of  
210 4.4 and 4.0 based on the H<sub>2</sub> and O<sub>2</sub> data, respectively. The good agreement between the results based  
211 on H<sub>2</sub> (D<sub>2</sub>) and O<sub>2</sub> detection show that the different solubility, diffusion coefficient and possibly  
212 different response of the electrochemical sensor to D<sub>2</sub> compared to H<sub>2</sub> do not significantly impact the  
213 measurement (as there would otherwise be a larger difference to the KIE based on the O<sub>2</sub> data, which  
214 is not affected by the switch from H<sub>2</sub>O to D<sub>2</sub>O). This rather large KIE would indicate that protons are  
215 involved in the rate determining step. This, however, is in contrast to a previous finding in the  
216 literature, where Lercher and co-workers reported a KIE of 1.1 based on GC measurements.<sup>[23]</sup> Due to  
217 this deviation we also performed analogous experiments with D<sub>2</sub>O and gas phase measurements (see  
218 Figure 3E). In this case, we found KIEs of 2.3 and 2.7 based on the H<sub>2</sub> and O<sub>2</sub> data, respectively. It is  
219 important to note that the maximum rates in the liquid and gas phase are observed on significantly  
220 different time scales: for liquid phase measurements the maximum rate is observed after ca. 300 s,

221 while for gas phase measurements the maximum rate is observed after ca. 3.000 – 4.000 s. These  
222 different scales might point to a way to rationalize the different KIEs obtained in liquid and gas phase  
223 measurements as well as the result from the literature: potentially, the rate determining step changes  
224 over the course of the reaction (e.g. due to different phases of catalyst activation/deactivation), with a  
225 rate determining step that involves protons in the initial reaction phase and a different rate determining  
226 step without proton involvement in the later reaction phase. This rationalization, however, is only a  
227 hypothesis for now and requires further investigations.

228

229 **Conclusion**

230 In summary, we report the design of a novel, open-source photoreactor set-up, which allows for  
231 reproducible overall water splitting experiments with *in situ* detection of H<sub>2</sub> and O<sub>2</sub> in both the liquid  
232 and gas phase. This layout allows for performing experiments under conditions that can be adapted to  
233 be analogous to scalable photoreactor systems, where the product gases accumulate in the gas phase.  
234 The presented measurement principle therefore gives *operando* insights which can be translated to  
235 application-scale systems. Furthermore, the high time resolution offers rich kinetic insights into the  
236 overall water splitting reaction, which cannot be obtained using slower/gas phase methods such as gas  
237 chromatography.

238 We established a robust workflow for processing the experimental data obtained using this set-up,  
239 yielding the maximum rates of H<sub>2</sub> and O<sub>2</sub> formation for both liquid and gas phase measurements. With  
240 the developed tools, we investigated the impacts of irradiance, temperature and co-catalyst loading on  
241 the maximum rates of overall water splitting using Rh<sub>2-y</sub>Cr<sub>y</sub>O<sub>3</sub>/Al:SrTiO<sub>3</sub> and could successfully  
242 reproduce previous observations from the literature. Interestingly, measuring the H/D kinetic isotope  
243 effect in the liquid phase (4.0 – 4.4) and gas phase (2.3 – 2.7) gave different results, both of which are  
244 higher than those previously reported based on GC measurements. Due to the different timescales of  
245 liquid and gas phase measurements this could possibly indicate a change in the rate determining step  
246 over the course of the reaction, but this hypothesis requires further investigation. Overall, the results  
247 highlight the versatility of the described approach for investigating overall photocatalytic water  
248 splitting, which will help advance progress in the field.

249

250 **Acknowledgments:** We gratefully acknowledge Michael Ringleb (FSU Jena) for support for printing  
251 of the irradiation chamber, as well as Florian David (FSU Jena) for building the reactor and double  
252 walled beaker. We would also like to express our gratitude to Dr. Lingli Ni for her assistance in  
253 carrying out the SEM/EDX measurements. Further we want to acknowledge Jens Ulbrich (FSU Jena)  
254 for technical support.

255 **Funding:** Financial support by Fonds der Chemischen Industrie (Liebig scholarship for J.S. and N.B.),  
256 Federal Ministry of Research, Technology and Space (BMFTR independent research group  
257 “SINATRA: SolSTEP”, grant number 03SF0729) and DFG via the CRC TRR 234 CATALIGHT  
258 (project no. 36454990, projects A7 and C6) is gratefully acknowledged.

259 **Author contributions:** Conceptualization: J.S.; investigation & data curation: N.B., A.E., E.A., D.K.;  
260 writing – original draft: N.B., A.E., J.S.; writing – review & editing: all authors; supervision: D.Z.,  
261 J.S.; resources: D.Z., J.S.; project administration: J.S.; funding acquisition: D.Z., J.S. All authors have  
262 read and agreed to the published version of the manuscript.

263 **Data availability:** Original data supporting the results of this study is available at:  
264 [https://github.com/water-splitting-group/o2\\_h2\\_reactor](https://github.com/water-splitting-group/o2_h2_reactor)

265 **Code availability:** Code developed for this study is available at:  
266 [https://github.com/jschneidewind/simultaneous\\_detection](https://github.com/jschneidewind/simultaneous_detection)

267 **Competing interests:** The author has no competing interests.

268 **Correspondence and requests for materials** should be addressed to J. S. (Jacob.Schneidewind@uni-  
269 jena.de).

270 **Supplementary Materials contains:**

271 Methods and Parameters

272 SI Figures

273 SI Tables

## References

- [1] B. A. Pinaud, J. D. Benck, L. C. Seitz, A. J. Forman, Z. Chen, T. G. Deutsch, B. D. James, K. N. Baum, G. N. Baum, S. Ardo, H. Wang, E. Miller, T. F. Jaramillo, “Technical and economic feasibility of centralized facilities for solar hydrogen production via photocatalysis and photoelectrochemistry” *Energy Environ. Sci.* **2013**, *6*, 1983–2002.
- [2] J. Schneidewind, “How Much Technological Progress is Needed to Make Solar Hydrogen Cost-Competitive?” *Adv. Energy Mater.* **2022**, *12*, 2200342.
- [3] H. Nishiyama, T. Yamada, M. Nakabayashi, Y. Maehara, M. Yamaguchi, Y. Kuromiya, Y. Nagatsuma, H. Tokudome, S. Akiyama, T. Watanabe, R. Narushima, S. Okunaka, N. Shibata, T. Takata, T. Hisatomi, K. Domen, “Photocatalytic solar hydrogen production from water on a 100-m<sup>2</sup> scale” *Nature* **2021**, *598*, 304–307.
- [4] F. Qin, Y. Kang, X. San, Y.-L. Tang, J. Li, X. Zhang, K. Zhang, G. Liu, “Spontaneous Exciton Dissociation in Sc-Doped Rutile TiO<sub>2</sub> for Photocatalytic Overall Water Splitting with an Apparent Quantum Yield of 30%” *J. Am. Chem. Soc.* **2025**, *147*, 12897–12907.
- [5] T. Takata, J. Jiang, Y. Sakata, M. Nakabayashi, N. Shibata, V. Nandal, K. Seki, T. Hisatomi, K. Domen, “Photocatalytic water splitting with a quantum efficiency of almost unity” *Nature* **2020**, *581*, 411–414.
- [6] J. Liu, Y. Liu, N. Liu, Y. Han, X. Zhang, H. Huang, Y. Lifshitz, S.-T. Lee, J. Zhong, Z. Kang, “Metal-free efficient photocatalyst for stable visible water splitting via a two-electron pathway” *Science* **2015**, *347*, 970–974.
- [7] T. Hisatomi, T. Yamada, H. Nishiyama, T. Takata, K. Domen, “Materials and systems for large-scale photocatalytic water splitting” *Nat. Rev. Mater.* **2025**, DOI 10.1038/s41578-025-00823-0.
- [8] S. Nishioka, F. E. Osterloh, X. Wang, T. E. Mallouk, K. Maeda, “Photocatalytic water splitting” *Nat. Rev. Methods Primer* **2023**, *3*, 1–15.
- [9] T. Takata, L. Lin, T. Hisatomi, K. Domen, “Best Practices for Assessing Performance of Photocatalytic Water Splitting Systems” *Adv. Mater.* **2024**, *36*, 2406848.
- [10] S. Nandy, T. Hisatomi, M. Nakabayashi, H. Li, X. Wang, N. Shibata, T. Takata, K. Domen, “Oxide layer coating enabling oxysulfide-based photocatalyst sheet to drive Z-scheme water splitting at atmospheric pressure” *Joule* **2023**, *7*, 1641–1651.
- [11] E. Kikuchi, N. Saito, Y. Yamaguchi, A. Kudo, “Temperature Dependence of Photocatalytic Water Splitting under Visible Light Irradiation over Ir- and Sb-Codoped SrTiO<sub>3</sub>:Al” *J. Phys. Chem. C* **2025**, *129*, 2381–2390.
- [12] F. L. Huber, S. Amthor, B. Schwarz, B. Mizaikoff, C. Streb, S. Rau, “Multi-phase real-time monitoring of oxygen evolution enables in operando water oxidation catalysis studies” *Sustain. Energy Fuels* **2018**, *2*, 1974–1978.
- [13] H. A. Vignolo-González, S. Laha, A. Jiménez-Solano, T. Oshima, V. Duppel, P. Schützendübe, B. V. Lotsch, “Toward Standardized Photocatalytic Oxygen Evolution Rates Using RuO<sub>2</sub>@TiO<sub>2</sub> as a Benchmark” *Matter* **2020**, *3*, 464–486.
- [14] L. Han, M. Lin, S. Haussener, “Reliable Performance Characterization of Mediated Photocatalytic Water-Splitting Half Reactions” *ChemSusChem* **2017**, *10*, 2158–2166.
- [15] L. Alibabaei, B. D. Sherman, M. R. Norris, M. K. Brennaman, T. J. Meyer, “Visible photoelectrochemical water splitting into H<sub>2</sub> and O<sub>2</sub> in a dye-sensitized photoelectrosynthesis cell” *Proc. Natl. Acad. Sci.* **2015**, *112*, 5899–5902.
- [16] W. S. dos Santos, M. Rodriguez, J. M. O. Khouri, L. A. Nascimento, R. J. P. Ribeiro, J. P. Mesquita, A. C. Silva, F. G. E. Nogueira, M. C. Pereira, “Bismuth Vanadate Photoelectrodes with High Photovoltage as Photoanode and Photocathode in Photoelectrochemical Cells for Water Splitting” *ChemSusChem* **2018**, *11*, 589–597.
- [17] D. Kowalczyk, P. Li, A. Abbas, J. Eichhorn, P. Buday, M. Heiland, A. Pannwitz, F. H. Schacher, W. Weigand, C. Streb, D. Ziegenbalg, “Making Photocatalysis Comparable Using a Modular and Characterized Open-Source Photoreactor” *ChemPhotoChem* **2022**, *6*, e202200044.

- 324 [18] A. Indra, P. W. Menezes, M. Driess, "Photocatalytic and photosensitized water splitting: A plea  
325 for well-defined and commonly accepted protocol" *Comptes Rendus Chim.* **2018**, *21*, 909–915.  
326 [19] Z. Wang, T. Hisatomi, R. Li, K. Sayama, G. Liu, K. Domen, C. Li, L. Wang, "Efficiency  
327 Accreditation and Testing Protocols for Particulate Photocatalysts toward Solar Fuel Production"  
328 *Joule* **2021**, *5*, 344–359.  
329 [20] Y. Ham, T. Hisatomi, Y. Goto, Y. Moriya, Y. Sakata, A. Yamakata, J. Kubota, K. Domen, "Flux-  
330 mediated doping of SrTiO<sub>3</sub> photocatalysts for efficient overall water splitting" *J. Mater. Chem.*  
331 *A* **2016**, *4*, 3027–3033.  
332 [21] Y. Goto, T. Hisatomi, Q. Wang, T. Higashi, K. Ishikiriyama, T. Maeda, Y. Sakata, S. Okunaka,  
333 H. Tokudome, M. Katayama, S. Akiyama, H. Nishiyama, Y. Inoue, T. Takewaki, T. Setoyama,  
334 T. Minegishi, T. Takata, T. Yamada, K. Domen, "A Particulate Photocatalyst Water-Splitting  
335 Panel for Large-Scale Solar Hydrogen Generation" *Joule* **2018**, *2*, 509–520.  
336 [22] Z. Zhao, R. V. Goncalves, S. K. Barman, E. J. Willard, E. Byle, R. Perry, Z. Wu, M. N. Huda, A.  
337 J. Moulé, F. E. Osterloh, "Electronic structure basis for enhanced overall water splitting  
338 photocatalysis with aluminum doped SrTiO<sub>3</sub> in natural sunlight" *Energy Environ. Sci.* **2019**, *12*,  
339 1385–1395.  
340 [23] K. E. Sanwald, T. F. Berto, A. Jentys, D. M. Camaioni, O. Y. Gutiérrez, J. A. Lercher, "Kinetic  
341 Coupling of Water Splitting and Photoreforming on SrTiO<sub>3</sub>-Based Photocatalysts" *ACS Catal.*  
342 **2018**, *8*, 2902–2913.  
343 [24] T. M. Rahman, D. J. Osborn, A. E. Pellicone, P. C. Tapping, T. Takata, T. Hisatomi, H.  
344 Nishiyama, K. Domen, G. G. Andersson, G. F. Metha, "Photocatalyst sheet performance under  
345 intense UV irradiation and increased temperatures" *EES Sol.* **2025**, *1*, 536–542.  
346 [25] T. Hisatomi, K. Maeda, K. Takanabe, J. Kubota, K. Domen, "Aspects of the Water Splitting  
347 Mechanism on (Ga<sub>1-x</sub>Zn<sub>x</sub>)(N<sub>1-x</sub>O<sub>x</sub>) Photocatalyst Modified with Rh<sub>2-y</sub>Cr<sub>y</sub>O<sub>3</sub> Cocatalyst"  
348 *J. Phys. Chem. C* **2009**, *113*, 21458–21466.  
349 [26] T. Hisatomi, K. Miyazaki, K. Takanabe, K. Maeda, J. Kubota, Y. Sakata, K. Domen, "Isotopic  
350 and kinetic assessment of photocatalytic water splitting on Zn-added Ga<sub>2</sub>O<sub>3</sub> photocatalyst loaded  
351 with Rh<sub>2</sub>–Cr O<sub>3</sub> cocatalyst" *Chem. Phys. Lett.* **2010**, *486*, 144–146.  
352